Adaptive Neural Network-Based Voltage Regulation for a High-Gain Boost Converter in Solar Photovoltaic Systems

Mohcine Byar [1*], Abdelouahed Abounada [2], Ghizlane Chbirik [3]
[1, 2, 3] Dept. of Electrical Engineering, Sultan Moulay Slimane University, Beni Mellal, Morocco
Email: [1] mohcinebyar2013@gmail.com, [2] a.abounada@gmail.com, [3] ghizlane.chbirik@gmail.com
*Corresponding Author

***Abstract*—This study proposes an adaptive Artificial Neural Network-based voltage control strategy for maintaining a stable DC bus voltage in a high-gain DC-DC boost converter for solar photovoltaic systems. Unlike conventional PID controllers, which struggle with non-linear and dynamic conditions, the proposed controller dynamically adjusts the duty cycle to mitigate the effects of varying solar irradiance and reference voltage, ensuring robust voltage regulation with reduced overshoot, enhanced transient response, and improved steady-state stability. This approach addresses critical challenges in standalone solar applications, such as water pumping and rural electrification, where consistent performance is essential despite fluctuating environmental conditions. In comparison to conventional control strategies, the ANN-based controller demonstrates superior adaptability, particularly under rapidly changing operating conditions. The results demonstrate the superior adaptability and efficiency of the ANN-based controller compared to the conventional PID controller, making it a valuable and reliable solution for sustainable solar PV systems. The proposed system was validated using a co-simulation framework that integrates MATLAB/Simulink and OrCAD, facilitating performance evaluation under varying solar irradiance and reference voltage conditions.**

Keywords*—Adaptive Voltage Control; Artificial Neural Network (ANN); High-Gain Boost Converter; DC Bus Voltage Regulation; Solar Photovoltaic Systems

I. Introduction

The increasing global reliance on renewable energy systems is driven by the environmental and economic challenges posed by fossil fuels [1]–[4]. Among various renewable sources, solar photovoltaic (PV) technology is widely adopted due to its scalability, minimal environmental impact, and potential for decentralized energy generation [5]–[8]. However, the intermittent nature of solar irradiance leads to significant fluctuations in power output, negatively affecting the stability and efficiency of PV systems [61]. Addressing these fluctuations requires advanced energy conversion and control strategies to ensure stable and reliable operation under varying environmental conditions [9]–[13].

High-gain boost converters (HGBCs) play a crucial role in modern PV systems by stepping up the low DC voltage generated by solar panels to higher levels with significantly improved voltage gain compared to conventional boost converters [14]–[16]. These converters utilize advanced circuit topologies, such as coupled inductors, switched capacitors, and voltage multipliers, which enable them to achieve higher voltage gains while operating at lower duty cycles [23]–[27]. This makes them essential in applications requiring high DC voltage, such as standalone systems and motor drives, where conventional boost converters struggle to provide sufficient gain without excessive switching losses and component stress [17]–[22]. However, ensuring precise voltage regulation in HGBCs remains challenging due to their complex and highly non-linear behavior under varying solar irradiance [28], [29].

Conventional controllers, particularly proportional-integral-derivative (PID) controllers, are widely used in photovoltaic systems for voltage regulation due to their simplicity and effectiveness under steady-state conditions [30]–[32]. However, their fixed control parameters and linear design limit their ability to handle rapid changes in solar irradiance and operating conditions. This often results in overshoot, oscillations, and prolonged settling times, leading to degraded performance in dynamic environments [33], [34]. Furthermore, extensive tuning of PID gains is required to optimize performance across varying conditions, making them less practical for real-world PV applications with fluctuating inputs [61].

In response to these challenges, artificial neural networks (ANN) have emerged as a promising solution for adaptive control in power electronics. ANNs are capable of modeling complex, non-linear system dynamics and predicting control actions in real time, allowing them to adapt to rapidly changing conditions [35]–[37]. ANN-based controller applications have demonstrated improvements in both transient response and steady-state accuracy, particularly in the tracking of maximum power points and other renewable energy applications [38]–[40]. Despite these advancements, limited research has focused on integrating ANN-based control strategies with high-gain boost converters, leaving a gap in addressing the unique challenges of dynamic voltage regulation in solar PV systems.

This study presents an adaptive ANN-based voltage control strategy for a HGBC in solar PV systems. The proposed controller dynamically adjusts the duty cycle to maintain a stable DC bus voltage, reducing transient overshoot, minimizing steady-state error, and enhancing system stability. Unlike conventional methods, the ANN-based approach eliminates the dependence on complex mathematical models, making it robust and adaptable to environmental fluctuations [41], [42].

The proposed control system is validated through a co-simulation framework integrating MATLAB/Simulink and OrCAD. This setup allows for a detailed evaluation of system performance under varying solar irradiance and reference voltage conditions, capturing both circuit-level non-linearities and control behavior [62]. The results demonstrate that the ANN-based controller significantly outperforms conventional PID control by achieving faster stabilization, reduced overshoot, and improved adaptability to disturbances.

This research makes several key contributions. First, the study develops an adaptive ANN-based control strategy specifically designed for a specific HGBC in solar PV systems. Second, it implements a comprehensive co-simulation framework combining MATLAB/Simulink and OrCAD to enable detailed performance evaluation under realistic operating conditions. Third, a comparative performance analysis demonstrates improved voltage regulation, enhanced transient response, and superior adaptability compared to conventional PID controllers. By addressing these challenges, this study advances intelligent control strategies for renewable energy systems, with potential applications in water pumping, rural electrification, and other standalone PV solutions.

II. Method

This section details the technical implementation of the proposed adaptive control strategy for the HGBC and its validation through co-simulation. Fig. 1 presents the synoptic diagram of the proposed system, which integrates a PV array, the HGBC, an ANN-based controller, and the DC load. The system employs a feedback control mechanism wherein the controller monitors the output voltage and dynamically adjusts the duty cycle to maintain stable voltage regulation under varying conditions.

A. Model of the High-Gain Boost Converter

HGBCs play a crucial role in PV systems by bridging the gap between the low output voltage of solar panels and the higher voltage demands of applications such as inverters, energy storage, and motor drives [43]–[46]. Unlike conventional boost converters, the HGBC achieves significant voltage amplification while minimizing component stress and switching losses. As shown in Fig. 2, the converter consists of three inductors (L_1, L_2, L_3), two capacitors (C_1, C_o), two diodes (D_1, D_o), and three switches (S_1, S_2, S_3). This configuration enables efficient operation in continuous conduction mode (CCM) [47], ensuring uninterrupted inductor current and stable energy transfer to the load.

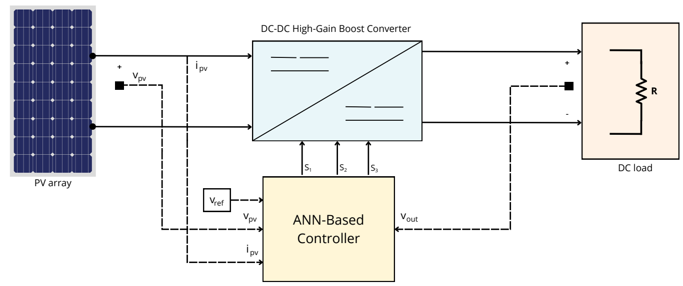

Fig. 1. Synoptic diagram of the proposed DC bus voltage regulation system using ANN control

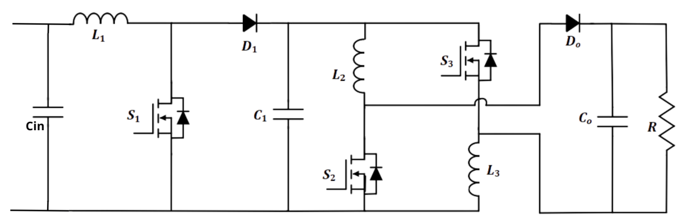

Fig. 2. Schematic of the proposed HGBC for photovoltaic applications.

The proposed system utilizes a Jinko JKM275PP-60 PV module, which provides a maximum power output of 275 W at a voltage of 32.0 V and a current of 8.61 A. The HGBC steps up this voltage to 350 V, with a duty cycle of 0.6 and a switching frequency of 30 kHz. The converter operates in two distinct phases: the switch-on phase, during which the inductors store energy, and the switch-off phase, where the stored energy is transferred to the output capacitor and load.

The component values of the HGBC are designed to ensure stable operation under continuous conduction mode while minimizing ripples in both inductor current and capacitor voltage. The inductor value is calculated to limit the ripple current to an acceptable level. Using the volt-second balance principle [63], the inductor value is determined by the following equation:

$$L = \frac{V_{in} \cdot D}{f_{sw} \cdot \Delta I_L} \tag{1}$$

Here, V_{in} is the input voltage, D is the duty cycle, f_{sw} is the switching frequency, and ΔI_L is the desired inductor ripple current. For the given system parameters, the inductor value is calculated to be 3 mH.

Similarly, the output capacitor value is determined based on the allowable ripple voltage at the output. The capacitor value is given by:

$$C = \frac{I_{out} \cdot D}{f_{sw} \cdot \Delta V_C} \tag{2}$$

In this equation, I_{out} is the output current, and ΔV_C is the allowed ripple voltage. **With the system's parameters, the capacitor value is designed to be 260 μF.** These values ensure that the converter maintains continuous conduction mode and stable voltage regulation with minimal ripple, improving overall system efficiency and reliability under fluctuating environmental conditions.

The voltage gain of the converter is described using the volt-second balance principle and is expressed as:

$$G = \frac{V_o}{V_{in}} = \frac{1 + D}{(1 - D)^2} \tag{3}$$

For the given duty cycle of 0.6, the expected voltage gain is computed as:

$$G = \frac{1 + 0.6}{(1 - 0.6)^2} = 10 \tag{4}$$

This confirms that the designed HGBC successfully increases the voltage of the photovoltaic module from 32V to the desired 350V, ensuring stable operation for DC loads.

B. ANN Controller Design and Training Process

The proposed ANN controller addresses the limitations of traditional controllers by dynamically adapting to non-linear and time-varying conditions. This adaptability is crucial in PV systems, where environmental variations such as irradiance and temperature fluctuations significantly affect performance [48]–[52]. The ANN's ability to approximate complex non-linear functions enhances the stability, efficiency, and voltage regulation of the system under dynamic scenarios. By leveraging this capability, the system can achieve more precise control than conventional techniques [64].

The ANN is designed as a three-layer feedforward network optimized for the HGBC [53], [54], [65]. The architecture consists of an input layer, two hidden layers, and an output layer. The input layer processes four critical signals: the reference voltage (V_{ref}), the measured output voltage (V_{out}), the photovoltaic array voltage (V_{pv}), and the error signal ($e = V_{ref} - V_{out}$). These inputs provide comprehensive real-time data, enabling precise voltage regulation by accurately modeling system dynamics. The hidden layers use the sigmoid activation function, defined by:

$$f(x) = \frac{1}{1 + e^{-x}} \tag{5}$$

This function was chosen for its effectiveness in modeling non-linear behavior, ensuring smooth transitions and stable control [66]. The number of neurons and layers was determined through iterative optimization to balance computational efficiency and model accuracy, minimizing the risk of both underfitting and overfitting [67]. Fig. 3 illustrates the ANN architecture used in this study.

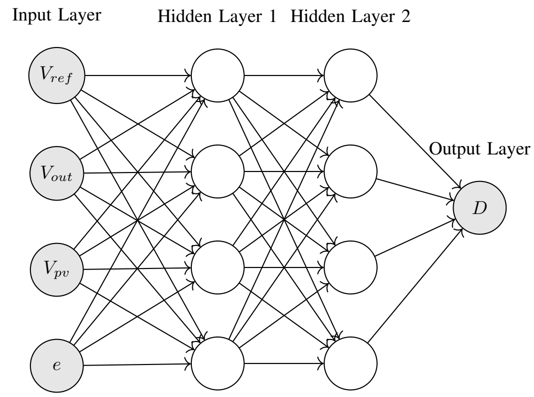

Fig. 3. ANN architecture for controlling the high-gain boost converter

To train the ANN, a dataset was generated by simulating various environmental and load conditions, including fluctuations in solar irradiance and PV voltage. The network's training objective was to minimize the error between the predicted and target duty cycle values, achieved through the backpropagation algorithm [56], [57]. The mean squared error (MSE) served as the objective function for training, where D_i and $\hat{D}_i$ denote the target and predicted duty cycles, respectively and it is defined by:

$$MSE = \frac{1}{n} \sum_{i=1}^{n} \left(D_i - \hat{D}_i \right)^2 \tag{6}$$

Hyperparameters such as the learning rate, number of neurons, and number of epochs were tuned through experimentation to optimize convergence speed and accuracy [68]. The training process was monitored using metrics such as MSE reduction between epochs and validation accuracy. Fig. 4 and Fig. 5 illustrate the training results, showing significant improvements in MSE throughout the training, validation, and test phases.

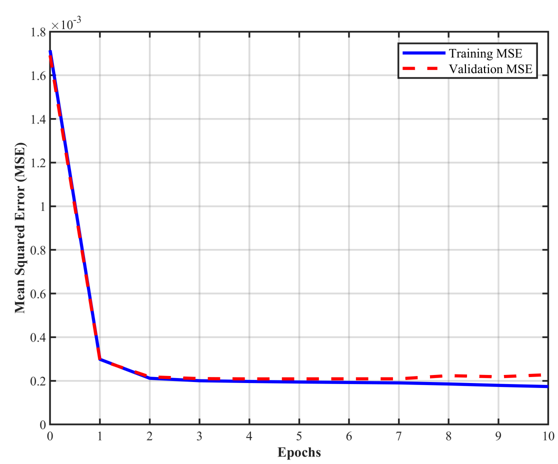

Fig. 4. Mean squared error (MSE) convergence during training.

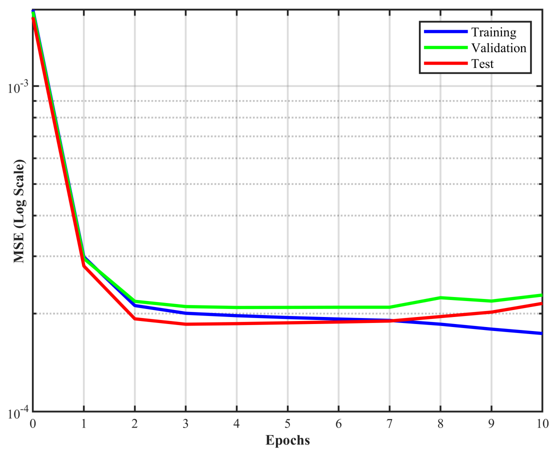

Fig. 5. Comparison of MSE across training, validation, and testing phases.

To enhance the clarity of the training methodology, a flowchart summarizing the process is provided in Fig. 6. This diagram details each stage, from data preparation to model validation.

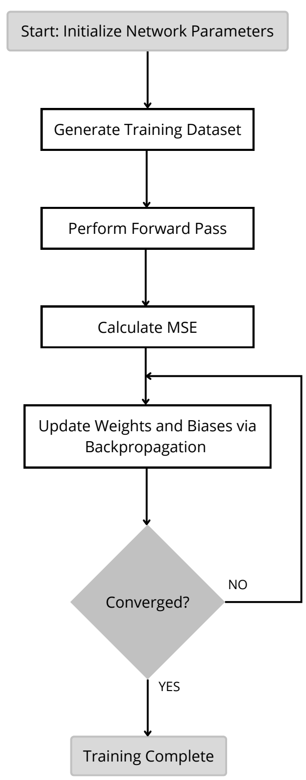

Fig. 6. Training process flowchart for the ANN-based control system.

C. Co-Simulation Framework

The proposed co-simulation framework was developed to address the need for accurate and realistic evaluation of both control strategies and circuit dynamics. This hybrid approach integrates MATLAB and OrCAD, combining the strengths of both platforms to achieve comprehensive system validation. MATLAB is chosen for control development because it excels in numerical simulations, ANN training, and algorithm optimization, while OrCAD offers detailed circuit modeling with non-ideal real-world components [59].

MATLAB employs ideal models for components and is optimized for control algorithm simulations. This makes it highly efficient for tasks such as training ANNs, optimizing performance, and fine-tuning control strategies. However, MATLAB's limitations in accurately capturing real-world circuit characteristics require an additional platform. OrCAD, on the other hand, provides a circuit simulation environment that accounts for real-world component behavior, including nonlinearities, switching losses, and parasitic elements [60]. By integrating both tools, the co-simulation framework bridges the gap between ideal control theory and practical circuit-level performance.

Through this integration, dynamic real-time data is exchanged between the control system and circuit model via the SLPS interface. Key control signals, such as the reference voltage (V_{ref}), output voltage (V_{out}), and error signal ($e = V_{ref} - V_{out}$), are communicated in both directions between MATLAB and OrCAD. This setup enables the ANN controller to interact with a realistic converter model in real-time, ensuring synchronized transient response and accurate steady-state performance assessment.

Environmental parameters, such as solar irradiance and temperature, are introduced in the OrCAD model to simulate realistic operating conditions. This allows the control system to be evaluated under dynamic scenarios, including rapid irradiance fluctuations and varying reference voltage demands, further enhancing reliability. Fig. 7 illustrates the co-simulation framework, showing the flow of control and circuit-level signals.

This co-simulation approach provides several advantages over standalone simulations in either platform. MATLAB simulations, while fast and efficient, may not fully reflect the practical limitations of real-world components. Conversely, OrCAD simulations alone may be computationally expensive and less efficient for control algorithm development. By combining the two, this framework ensures that both control and circuit behaviors are validated in a synchronized manner.

Finally, this framework allows us to verify the ANN controller's ability to regulate the output voltage, minimize transient overshoots, and achieve fast settling times under real-world conditions. This integration strengthens confidence in the controller's performance and reliability before potential real-time hardware implementation.

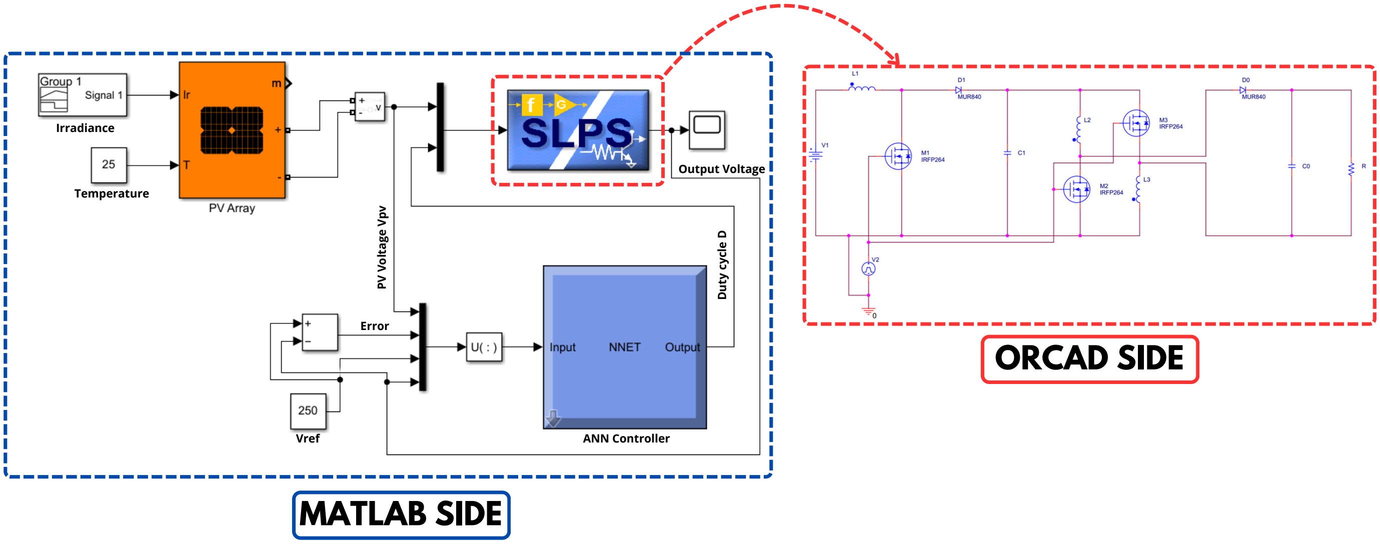

Fig. 7. Co-simulation framework integrating MATLAB and OrCAD for ANN-based control system validation.

III. Results and Discussion

The performance of the proposed HGBC and its adaptive ANN-based controller is critically analyzed through extensive simulations under various operating conditions. This analysis is designed to emulate realistic scenarios encountered by PV systems, including fluctuations in solar irradiance and changes in reference voltage. The results provide a comprehensive assessment of the system's transient and steady-state behavior, focusing on key performance indicators such as voltage stability, response time, and control adaptability. These metrics are pivotal in determining the reliability and efficiency of the converter in dynamic environments, where conventional controllers often face limitations.

The photovoltaic module used in this study, the Jinko Solar JKM275PP-60, is rated at 275 W under standard test conditions (STC). Its selection was based on a balance between performance reliability and efficiency, aligned with standard practices for the evaluation of the PV system.

The electrical parameters of the PV module and the specifications of the HGBC components were optimized to minimize ripple, improve the transient response and maintain steady-state stability. Table I presents these key parameters, which form the basis for evaluating the performance of the system under various operating conditions. The component choices, particularly for inductors, capacitors and MOSFET switches, were based on trade-offs between switching frequency, voltage gain, and energy storage requirements.

The analysis includes a comparative evaluation of the proposed ANN-based controller and a conventional PID controller. The comparison focuses on critical performance metrics such as rise time, overshoot, settling time, and steady-state error. These metrics are essential for ensuring stable and efficient system operation under fluctuating environmental conditions. While the PID controller's fixed-gain structure limits its adaptability to nonlinear system dynamics, the ANN leverages its training on varying input scenarios to dynamically adjust the control strategy, resulting in superior performance in both transient and steady-state responses.

TABLE I. Key Parameters of the PV Module and Boost Converter

Component	Value
Photovoltaic Module (Jinko JKM275PP-60)	
Maximum Power (P_{max})	275 W
Voltage at P_{max} (V_{mp})	32.0 V
Current at P_{max} (I_{mp})	8.61 A
Open Circuit Voltage (V_{oc})	38.7 V
Short Circuit Current (I_{sc})	9.38 A
Boost Converter Components	
Inductors (L_1, L_2, L_3)	3 mH each
Capacitors (C_{in}, C_1, C_o)	260 μF each
Switches (S_1, S_2, S_3)	IRFP264 MOSFET
Diodes (D_1, D_o)	MUR840

A. Constant Irradiance with Constant Reference Voltage

Fig. 8 illustrates the response to the output voltage of the HGBC during startup under a constant solar irradiance of 1000 W/m^2 and a reference voltage of 250 V. In this scenario, the duty cycle is set to approximately 0.6 to achieve the required voltage gain. ANN and PID controllers are compared based on their ability to regulate output voltage, focusing on key metrics such as rise time, overshoot, and settling time, as summarized in Table II.

The ANN controller rapidly stabilizes the output voltage, achieving an increase time of 109.62 ms, with a minimal overshoot of 1.53% (3.83 V) and a settle time of 0.39 s. This performance is attributed to the ANN's real-time prediction and adjustment capabilities, which dynamically regulate the duty cycle to match the system's energy transfer needs. ANN efficiently manages inductor charging and capacitor stabilization, preventing large voltage spikes during transient conditions.

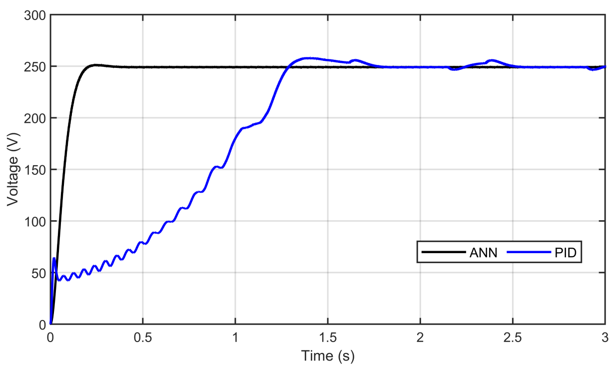

Fig. 8. Output voltage waveform during start-up at STC and 250 V reference.

TABLE II. PERFORMANCE METRICS COMPARISON OF ANN AND PID CONTROLLERS

Metric	*ANN Controller*	*PID Controller*
Rise Time (ms)	**109.62**	**820.88**
Overshoot (%)	**1.53**	**4.48**
Overshoot (Volts)	**3.83**	**11.2**
Settling Time (s)	**0.39**	**Not Settling**

In contrast, the PID controller exhibits an increase time of 828.88 ms and an overshoot of 4.48% (11.2 V), failing to settle within the observation period. This inferior performance is primarily due to the static gain parameters of the PID, which cannot adapt to the highly non-linear behavior of the HGBC. As a result, the controller struggles to mitigate rapid changes in inductor current, causing prolonged instability and oscillatory behavior.

The voltage waveform in Fig. 8 highlights the superior transient response of the ANN controller, characterized by a smooth trajectory toward the reference voltage with negligible oscillations. In contrast, the PID controller exhibits significant overshoot and oscillation during the start-up phase, reflecting its inability to handle complex nonlinearities without extensive tuning.

The ANN's performance improvement over PID control is further evidenced by the steady-state error reduction. By continuously adapting its control parameters based on system feedback, the ANN minimizes both transient and steady-state deviations, demonstrating robust voltage regulation under constant operating conditions.

The results presented here demonstrate the superior capability of the ANN controller in dynamic regulation under constant conditions. The next subsection examines how both controllers perform under variable reference voltage conditions.

B. Dynamic Voltage Transitions under Constant Irradiance

The system's transient and steady-state performance is assessed under constant solar irradiance of 1000 W/m^2, with the reference voltage varied between 250 V, 200 V, and 220 V. This test emulates operational scenarios where reference voltage adjustments are necessary to accommodate fluctuating demands in PV applications. The output voltage profiles during these transitions are shown in Fig. 9.

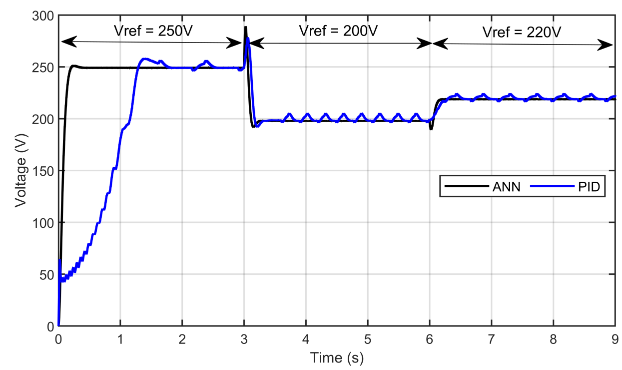

Fig. 9. Output voltage response for varying reference voltages at 1000 W/m^2 irradiance.

During the transition from 250V to 200V, the ANN controller achieves an overshoot of 15.48% (30.96V), a settling time of 0.408s, and a steady-state error of 1.5V. This overshoot results from the sudden release of stored inductor and capacitor energy, which momentarily exceeds the target voltage. The ANN promptly adjusts the duty cycle, minimizing oscillations and restoring stability. This rapid convergence highlights the predictive capabilities of ANN in adapting to non-linear system variations through real-time feedback.

On the other hand, the PID controller faces significant performance degradation, with an overshoot of 39.25% (78.5 V) and prolonged instability. Its static gain structure impairs the response time, preventing effective error correction. The accumulated error of the integral term delays the adjustment of the control signal, while the proportional term excessively amplifies deviations, leading to sustained oscillations.

The transition from 200V to 220V further underscores the adaptability of the ANN controller. It maintains zero overshoot, a settling time of 0.22s, and a minimal steady-state error of 0.4V. This performance demonstrates the ability of the ANN to anticipate and counteract rapid changes in system voltage, ensuring stable energy transfer and output regulation. In contrast, the PID controller experiences an overshoot of 28.08% (56.16V) and remains unable to achieve stability, emphasizing its limited capacity to handle dynamic transitions effectively.

The voltage waveforms in Fig. 9 highlight the smooth regulation achieved by the ANN controller, with minimal oscillations and rapid convergence to the reference voltage. In contrast, the PID controller shows erratic voltage swings and delayed error correction, emphasizing its limitations in managing dynamic transitions.

These findings, summarized in Table III, confirm the superiority of the ANN controller to handle rapid voltage changes. Its adaptive response minimizes both transient and steady-state errors, making it a reliable solution for real-time PV applications that require dynamic voltage regulation.

TABLE III. PERFORMANCE METRICS UNDER VARIABLE REFERENCE VOLTAGES

Reference Voltage (V)	**250**	**200**	**220**
ANN Controller			
Overshoot (%)	**1.53**	**15.48**	**0**
Overshoot (V)	**3.83**	**30.96**	**0**
Settling Time (s)	**0.109**	**0.408**	**0.22**
Steady-State Error (V)	**2.0**	**1.5**	**0.4**
PID Controller			
Overshoot (%)	**3.44**	**39.25**	**28.08**
Overshoot (V)	**8.6**	**78.5**	**56.16**
Settling Time (s)	**Not Settling**	**Not Settling**	**Not Settling**
Steady-State Error (V)	**1.9**	**5.4**	**4.65**

C. Dynamic Irradiance with Constant Reference Voltage

The system's voltage regulation is evaluated under dynamic solar irradiance conditions while maintaining a constant reference voltage of 250 V. Irradiance levels were varied between 1000 W/m^2, 500 W/m^2, and 800 W/m^2, simulating real-world conditions such as partial shading and passing clouds. This analysis aims to assess how both controllers handle transient and steady-state responses during fluctuating input power.

The voltage profiles during these transitions are illustrated in Fig. 10, with performance metrics summarized in Table IV. The ANN controller exhibits strong adaptability at all irradiance levels, with rapid stabilization and minimal overshoot. Its dynamic regulation is achieved by continuous adjustments to the duty cycle, ensuring efficient energy transfer and steady-state accuracy.

Under an irradiance drop to 500 W/m^2, the ANN controller achieves a settling time of 0.315 s and a steady-state error of 5.4 V. This performance is attributed to the ANN's capacity to recalibrate based on reduced input power, maintaining voltage regulation by efficiently compensating for lower energy availability. On the other hand, the PID controller is unable to stabilize under this condition, with a steady-state error of 2.1 V. Its inability to adapt to sudden changes in input power results in oscillations and prolonged instability.

At 800 W/m^2, the ANN controller continues to demonstrate optimal control, achieving zero overshoot, a settling time of 0.22 s, and a minimal steady-state error of 1.1 V. This reflects the ANN's ability to generalize effectively across various input conditions, even when such conditions were not explicitly part of its training. In contrast, the PID controller records an overshoot of 3.08% (7.7 V) and remains unstable, underscoring the limitations of fixed-gain control in dynamic environments.

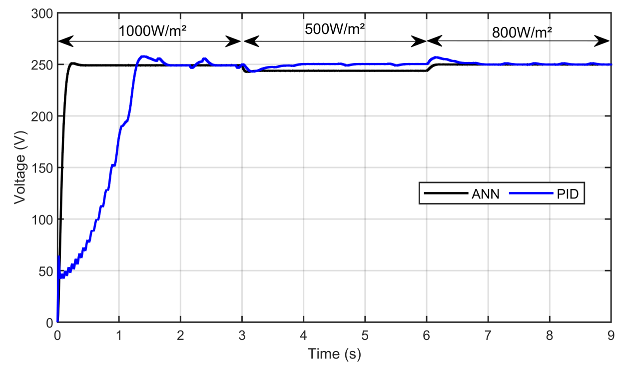

Fig. 10. Output voltage waveform under varying irradiance conditions and a constant reference voltage of 250 V.

TABLE IV. PERFORMANCE METRICS UNDER VARIABLE IRRADIANCE CONDITIONS

Irradiance (W/m^2)	1000	500	800
ANN Controller			
Overshoot (%)	1.53	0	0
Overshoot (V)	3.83	0	0
Settling Time (s)	0.39	0.315	0.22
Steady-State Error (V)	1.8	5.4	1.1
PID Controller			
Overshoot (%)	4.49	0	3.08
Overshoot (V)	11.22	0	7.7
Settling Time (s)	Not Settling	Not Settling	Not Settling
Steady-State Error (V)	2.0	2.1	1.1

The voltage waveforms in Fig. 10 clearly demonstrate the ANN's superior transient response, characterized by smooth convergence to the reference voltage without oscillations. By comparison, the PID controller struggles with erratic swings, unable to adjust control parameters rapidly enough to mitigate disturbances.

These observations reinforce the ANN controller's reliability and efficiency in real-time PV applications where fluctuating environmental conditions are prevalent. The next subsection examines the system's behavior under simultaneous changes in both irradiance and reference voltage.

D. Combined Irradiance and Reference Voltage Variations

The adaptability of the system is evaluated under simultaneous changes in solar irradiance and reference voltage, simulating dynamic real-world scenarios. Irradiance levels were varied between 700 W/m^2, 500 W/m^2, and 800 W/m^2, while reference voltages were adjusted to 250 V, 200 V, and 220 V, respectively. This test examines how well the ANN and PID controllers can regulate the output voltage under fluctuating environmental and operational conditions. The voltage profiles are shown in Fig. 11, and key performance metrics are summarized in Table V.

At 700 W/m^2 and a reference voltage of 250 V, the ANN controller achieves zero overshoot, a settling time of 0.465 s, and a steady-state error of 1.3 V. This performance highlights the ANN's ability to dynamically adapt the duty cycle, maintaining precise control over energy transfer despite fluctuating input power. The absence of overshoot demonstrates effective synchronization between inductor charging and output voltage stabilization. Conversely, the PID controller records an overshoot of 2.08% and fails to settle, underscoring its limited capability to address the non-linear and rapidly changing dynamics of the system.

During the transition to 500 W/m^2 and 200 V, the ANN exhibits a transient overshoot of 16.1% (32.2V) and a settling time of 0.296s. This temporary overshoot is a result of the system's internal energy rebalancing as it adapts to the reduced irradiance. The ANN's rapid recalibration minimizes oscillations, leading to swift stabilization with a steady-state error of 3.6V. In contrast, the PID controller struggles with severe performance degradation, failing to stabilize and exhibiting a steady-state error of 4.65 V. Its static gain configuration exacerbates instability when faced with simultaneous irradiance and voltage changes.

Under 800 W/m^2 and 220 V, the ANN controller once again demonstrates optimal performance, achieving zero overshoot, a settling time of 0.239 s, and a steady-state error of 2.9 V. This result confirms the ANN's robustness in managing dynamic conditions through continuous real-time adjustments. The controller efficiently balances input power variations and reference voltage demands, ensuring stable output regulation. By contrast, the PID controller remains unstable, unable to respond adequately to the changing parameters, further highlighting its limitations in adaptive control scenarios.

The voltage profiles in Fig. 11 clearly illustrate the ANN's smooth regulation, with rapid convergence to the target voltage and minimal oscillations. In contrast, the PID controller shows erratic swings and persistent instability, indicating its failure to manage dynamic interactions between input power and output voltage effectively.

These findings underscore the ANN controller's superior adaptability in handling complex, real-time operating conditions. Its enhanced transient and steady-state performance positions it as a reliable solution for PV systems that experience simultaneous environmental and operational fluctuations.

The performance evaluation confirms the superiority of the ANN controller in regulating output voltage under both constant and dynamic conditions. Its ability to predict and adapt to non-linear system variations enabled faster stabilization, reduced overshoot, and minimal steady-state error. In contrast, the static gain structure of the PID controller led to significant overshoot, prolonged instability, and failure to settle under rapidly changing conditions.

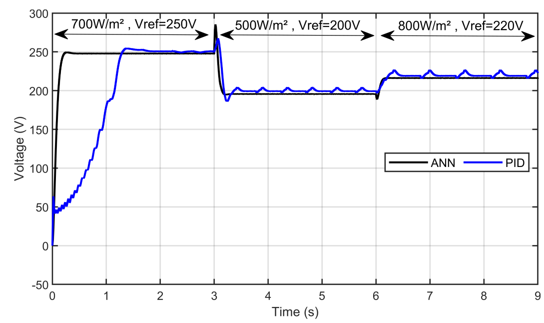

Fig. 11. Output voltage under combined irradiance and reference voltage variations.

TABLE V. PERFORMANCE METRICS OF ANN AND PID CONTROLLERS UNDER VARIABLE IRRADIANCE AND REFERENCE VOLTAGE

Metric	ANN (250V, 700 W/m^2)	ANN (200V, 500 W/m^2)	ANN (220V, 800 W/m^2)
Overshoot (%)	**0**	**16.1**	**0**
Settling Time (s)	**0.465**	**0.296**	**0.239**
Steady-State Error (V)	**1.3**	**3.6**	**2.9**
Metric	**PID (250V, 700 W/m^2)**	**PID (200V, 500 W/m^2)**	**PID (220V, 800 W/m^2)**
Overshoot (%)	**2.08**	**Not settling**	**Not settling**
Settling Time (s)	**Not settling**	**Not settling**	**Not settling**
Steady-State Error (V)	**1.8**	**4.65**	**7.1**

The ANN controller demonstrated resilience across all scenarios but showed transient overshoot during rapid reference voltage drops, highlighting a limitation in handling extreme transitions. This performance depends on the quality of the training data, which may need to be expanded for greater adaptability. Additionally, ANN controllers have higher computational demands compared to PID control, which can be a constraint in resource-limited systems.

The co-simulation framework integrated MATLAB/Simulink and OrCAD to accurately capture both control dynamics and circuit non-linearities, providing realistic performance validation. These findings establish the ANN controller as a reliable solution for real-world photovoltaic applications, offering enhanced voltage stability and system efficiency under varying environmental conditions. Future improvements could involve hybrid control strategies or dynamic retraining to further optimize performance.

IV. CONCLUSION

This study presented an adaptive ANN-based voltage control strategy for a HGBC in PV systems. Simulated under dynamic conditions using a MATLAB/OrCAD co-simulation platform, the ANN controller outperformed a conventional PID controller by achieving faster stabilization, reduced overshoot, and minimal steady-state errors. This demonstrates the ANN's adaptability to complex nonlinear system dynamics, making it suitable for real-world PV applications.

Although the ANN controller exhibited strong performance, occasional transient overshoot during rapid transitions highlights a need for further refinement. Furthermore, its reliance on extensive training data and computational complexity pose challenges for large-scale deployment. Future enhancements could include hybrid control strategies and reinforcement learning to improve scalability and efficiency.

Future work will focus on experimental validation and expanding the training dataset to cover extreme operating conditions. These improvements will strengthen the reliability of ANN, offering a robust and efficient solution for next-generation photovoltaic systems in dynamic environments.

REFERENCES

[1] A. I. Osman *et al.*, "Cost, environmental impact, and resilience of renewable energy under a changing climate: a review," *Environmental Chemistry Letters*, vol. 21, pp. 741–764, 2023, doi: 10.1007/s10311-022-01532-8.

[2] S. Algarni *et al.*, "Contribution of renewable energy sources to the environmental impacts and economic benefits for sustainable development," *Sustainable Energy Technologies and Assessments*, vol. 56, 2023, doi: 10.1016/j.seta.2023.103098.

[3] A. Raihan *et al.*, "The dynamic impacts of economic growth, financial globalization, fossil fuel, renewable energy, and urbanization on load capacity factor in Mexico," *Sustainability*, vol. 15, no. 18, 2023, doi: 10.3390/su151813462.

[4] F. Al Mubarak, R. Rezaee, and D. A. Wood, "Economic, societal, and environmental impacts of available energy sources: a review," *Engineering*, vol. 5, pp. 1232–1265, 2024, doi: 10.3390/eng5030067.

[5] A. Zisos, D. Chatzopoulos, and A. Efstratiadis, "The Concept of Spatial Reliability Across Renewable Energy Systems—An Application to Decentralized Solar PV Energy," *Energies*, vol. 17, 2024, doi: 10.3390/en17235900.

[6] Md H. Kabir, S. M. S. Newaz, T. Kabir, and A. S. Howlader, "Integrating Solar Power with Existing Grids: Strategies, Technologies, and Challenges & Review," *International Journal of Science and Engineering*, vol. 1, no. 2, pp. 48–62, 2024, doi: 10.62304/ijse.v1i2.142.

[7] E. Bullich-Massagué *et al.*, "A review of energy storage technologies for large scale photovoltaic power plants," *Applied Energy*, vol. 274, 2020, doi: 10.1016/j.apenergy.2020.115213.

[8] P. Nikolaidis, "Solar Energy Harnessing Technologies towards De-Carbonization: A Systematic Review of Processes and Systems," *Energies*, vol. 16, 2023, doi: 10.3390/en16176153.

[9] N. Mlilo, J. Brown, and T. Ahfock, "Impact of intermittent renewable energy generation penetration on the power system networks – A review," *Technology and Economics of Smart Grids and Sustainable Energy*, vol. 6, 2021, doi: 10.1007/s40866-021-00123-w.

[10] O. A. Al-Shahri *et al.*, "Solar photovoltaic energy optimization methods, challenges and issues: A comprehensive review," *Journal of Cleaner Production*, vol. 284, 2021, doi: 10.1016/j.jclepro.2020.125465.

[11] M. S. Hossain, N. A. Madlool, A. W. Al-Fatlawi, and M. El Haj Assad, "High Penetration of Solar Photovoltaic Structure on the Grid System Disruption: An Overview of Technology Advancement," *Sustainability*, vol. 15, 2023, doi: 10.3390/su15021174.

[12] T. S. Babu, K. R. Vasudevan, V. K. Ramachandaramurthy, S. B. Sani, S. Chemud, and R. M. Lajim, "A Comprehensive Review of Hybrid Energy Storage Systems: Converter Topologies, Control Strategies and Future Prospects," *IEEE Access*, vol. 8, pp. 148702–148721, 2020, doi: 10.1109/ACCESS.2020.3015919.

[13] Y. Zhou *et al.*, "Passive and active phase change materials integrated building energy systems with advanced machine-learning based climate-adaptive designs, intelligent operations, uncertainty-based analysis and optimisations: A state-of-the-art review," *Renewable and Sustainable Energy Reviews*, vol. 130, 2020, doi: 10.1016/j.rser.2020.109889

[14] T. Sutikno, H. S. Purnama, N. S. Widodo, S. Padmanaban, and M. R. Sahid, "A review on non-isolated low-power DC–DC converter topologies with high output gain for solar photovoltaic system applications," *Clean Energy*, vol. 6, no. 4, pp. 557–572, 2022, doi: 10.1093/ce/zkac037.

[15] F. Mumtaz *et al.*, "Review on non-isolated DC-DC converters and their control techniques for renewable energy applications," *Ain Shams Engineering Journal*, vol. 12, no. 4, pp. 3747–3763, 2021, doi: 10.1016/j.asej.2021.03.022.

[16] M. Hawsawi, H. M. D. Habbi, E. Alhawsawi, M. Yahya, and M. A. Zohdy, "Conventional and Switched Capacitor Boost Converters for Solar PV Integration: Dynamic MPPT Enhancement and Performance Evaluation," *Designs*, vol. 7, no. 5, 2023, doi: 10.3390/designs7050114.

[17] A. F. de Souza, F. L. Tofoli, and E. R. Ribeiro, "Switched Capacitor DC-DC Converters: A Survey on the Main Topologies, Design Characteristics, and Applications," *Energies*, vol. 14, 2021, doi: 10.3390/en14082231.

[18] P. S. Divya, N. Sathik, J. A. L., K. V., and D. Almakhles, "A comprehensive study on various DC–DC converter voltage-boosting topologies and their applications," *Circuit World*, vol. 48, no. 4, pp. 529–549, 2022, doi: 10.1108/CW-12-2020-0338.

[19] F. Alhaj Omar, "Comprehensive Analysis and Evaluation of DC-DC Converters: Advancements, Applications, and Challenges," *Black Sea Journal of Engineering and Science*, vol. 6, no. 4, pp. 557–571, 2023, doi: 10.34248/bsengineering.1357849.

[20] D. Nayanasiri and Y. Li, "Step-Down DC–DC Converters: An Overview and Outlook," *Electronics*, vol. 11, 2022, doi: 10.3390/electronics11111693.

[21] K. Zaoskoufis and E. C. Tatakis, "An Improved Boost-Based DC/DC Converter With High-Voltage Step-Up Ratio for DC Microgrids," *IEEE Journal of Emerging and Selected Topics in Power Electronics*, vol. 9, no. 2, pp. 1837–1853, 2021, doi: 10.1109/JESTPE.2020.2981018.

[22] T. Kobaku, R. Jeyasenthil, S. Sahoo, R. Ramchand, and T. Dragicevic, "Quantitative Feedback Design-Based Robust PID Control of Voltage Mode Controlled DC-DC Boost Converter," *IEEE Transactions on Circuits and Systems II: Express Briefs*, vol. 68, no. 1, pp. 286–290, 2021, doi: 10.1109/TCSII.2020.2988319.

[23] F. Yi and F. Wang, "Review of Voltage-Bucking/Boosting Techniques, Topologies, and Applications," *Energies*, vol. 16, 2023, doi: 10.3390/en16020842.

[24] M. Haris, M. Asim, and M. Tariq, "A Review of Non-Isolated High Gain DC-to-DC Converter Topologies," in *2022 2nd International Conference on Emerging Frontiers in Electrical and Electronic Technologies (ICEFEET)*, pp. 1–6, 2022, doi: 10.1109/ICEFEET51821.2022.9847767.

[25] B. T. Rao and D. De, "A Coupled Inductor-Based High-Gain ZVS DC–DC Converter With Reduced Voltage Stresses," *IEEE Transactions on Power Electronics*, vol. 38, no. 12, pp. 15956–15967, 2023, doi: 10.1109/TPEL.2023.3310577.

[26] M. Kumar, V. K. Yadav, and A. K. Verma, "Switched Capacitor Based High Gain Boost Converter for Renewable Energy Application," *IEEE Journal of Emerging and Selected Topics in Industrial Electronics*, vol. 4, no. 3, pp. 818–826, 2023, doi: 10.1109/JESTIE.2023.3262451.

[27] M. Rezaie and V. Abbasi, "Effective combination of quadratic boost converter with voltage multiplier cell to increase voltage gain," *IET Power Electronics*, vol. 13, no. 11, pp. 2322–2333, 2020, doi: 10.1049/iet-pel.2019.1070.

[28] X. Fan, H. Sun, Z. Yuan, Z. Li, R. Shi, and N. Ghadimi, "High Voltage Gain DC/DC Converter Using Coupled Inductor and VM Techniques," *IEEE Access*, vol. 8, pp. 131975–131987, 2020, doi: 10.1109/ACCESS.2020.3002902.

[29] Y. Guan, C. Cecati, J. M. Alonso, and Z. Zhang, "Review of High-Frequency High-Voltage-Conversion-Ratio DC–DC Converters," *IEEE Journal of Emerging and Selected Topics in Industrial Electronics*, vol. 2, no. 4, pp. 374–389, 2021, doi: 10.1109/JESTIE.2021.3051554.

[30] M. Q. Ademola and M. A. Idowu, "The Advent of the Proportional Integral Derivative Controller: A Review," *Technology*, vol. 2, 2023, doi: 10.24412/2181-1431-2023-2-5-22.

[31] R. P. Borase, D. K. Maghade, S. Y. Sondkar, et al., "A review of PID control, tuning methods and applications," *International Journal of Dynamics and Control*, vol. 9, pp. 818–827, 2021, doi: 10.1007/s40435-020-00665-4.

[32] G. Nethaji and J. Kathirvelan, "Performance comparison between PID and Fuzzy Logic Controllers for the hardware implementation of traditional high voltage DC-DC boost converter," *Heliyon*, vol. 10, no. 17, 2024, doi: 10.1016/j.heliyon.2024.e36750.

[33] G. C. Konstantopoulos and P. R. Baldivieso-Monasterios, "State-limiting PID controller for a class of nonlinear systems with constant uncertainties," *International Journal of Robust and Nonlinear Control*, vol. 30, no. 5, pp. 1770–1787, 2020, doi: 10.1002/rnc.4853.

[34] M. M. Sati, D. Kumar, A. Singh, M. Raparthi, F. Y. Alghayadh, and M. Soni, "Two-Area Power System with Automatic Generation Control Utilizing PID Control, FOPID, Particle Swarm Optimization, and Genetic Algorithms," in *2024 Fourth International Conference on Advances in Electrical, Computing, Communication and Sustainable Technologies (ICAECT)*, pp. 1–6, 2024, doi: 10.1109/ICAECT60202.2024.10469671.

[35] I. Alhamrouni, N. H. Abdul Kahar, M. Salem, M. Swadi, Y. Zahroui, D. J. Kadhim, F. A. Mohamed, and M. Alhuyi Nazari, "A Comprehensive Review on the Role of Artificial Intelligence in Power System Stability, Control, and Protection: Insights and Future Directions," *Applied Sciences*, vol. 14, 2024, doi: 10.3390/app14146214.

[36] M. Harib, H. Chaoui, and S. Miah, "Evolution of adaptive learning for nonlinear dynamic systems: a systematic survey," *Intelligent Robotics*, vol. 2, pp. 37–71, 2022, doi: 10.20517/ir.2021.19.

[37] A. Hashemi, G. Orzechowski, A. Mikkola, et al., "Multibody dynamics and control using machine learning," *Multibody System Dynamics*, vol. 58, pp. 397–431, 2023, doi: 10.1007/s11044-023-09884-x.

[38] S. Zhao, F. Blaabjerg, and H. Wang, "An Overview of Artificial Intelligence Applications for Power Electronics," *IEEE Transactions on Power Electronics*, vol. 36, no. 4, pp. 4633–4658, 2021, doi: 10.1109/TPEL.2020.3024914.

[39] T. B. Lopez-Garcia, A. Coronado-Mendoza, and J. A. Domínguez-Navarro, "Artificial neural networks in microgrids: A review," *Engineering Applications of Artificial Intelligence*, vol. 95, 2020, doi: 10.1016/j.engappai.2020.103894.

[40] A. Ramadevi *et al*., "Optimal Design and Performance Investigation of Artificial Neural Network Controller for Solar-and Battery-Connected Unified Power Quality Conditioner," *International Journal of Energy Research*, vol. 2023, no. 1, 2023, doi: 10.1155/2023/3355124.

[41] J. Krzywanski, M. Sosnowski, K. Grabowska, A. Zylka, L. Lasek, and A. Kijo-Kleczkowska, "Advanced Computational Methods for Modeling, Prediction and Optimization—A Review," *Materials*, vol. 17, 2024, doi: 10.3390/ma17143521.

[42] A. G. Olabi *et al*., "Artificial neural networks applications in partially shaded PV systems," *Thermal Science and Engineering Progress*, vol. 37, 2023, doi: 10.1016/j.tsep.2022.101612.

[43] C. B. Ali, A. H. Khan, K. Pervez, T. M. Awan, A. Noorwali, and S. A. Shah, "High Efficiency High Gain DC-DC Boost Converter Using PID Controller for Photovoltaic Applications," in *2021 International Congress of Advanced Technology and Engineering (ICOTEN)*, pp. 1–7, 2021, doi: 10.1109/ICOTEN52080.2021.9493476.

[44] M. M. S. Sulong *et al*., "Design and Simulation of High Gain DC-DC Boost Converter System for PV Application," in *2021 4th International Iraqi Conference on Engineering Technology and Their Applications (IICETA)*, pp. 179–183, 2021, doi: 10.1109/IICETA51758.2021.9717915.

[45] J. Ahmad, M. Zaid, A. Sarwar, C.-H. Lin, M. Asim, R. K. Yadav, M. Tariq, K. Satpathi, and B. Alamri, "A New High-Gain DC-DC Converter with Continuous Input Current for DC Microgrid Applications," *Energies*, vol. 14, 2021, doi: 10.3390/en14092629.

[46] W. Hassan *et al*., "Design, analysis and experimental verification of a high voltage gain and high-efficiency DC–DC converter for photovoltaic applications," *IET Renewable Power Generation*, vol. 14, no. 10, pp. 1699–1709, 2020, doi: 10.1049/iet-rpg.2019.1020.

[47] R. W. Erickson and D. Maksimović, "The Discontinuous Conduction Mode," in *Fundamentals of Power Electronics*, 2020, doi: 10.1007/978-3-030-43881-4_5.

[48] A. W. Khawaja *et al*., "Angle stability improvement using optimised proportional integral derivative with filter controller," *Heliyon*, vol. 10, no. 19, 2024, doi: 10.1016/j.heliyon.2024.e38944.

[49] A. Daraz, S. A. Malik, A. T. Azar, S. Aslam, T. Alkhalifah, and F. Alturise, "Optimized Fractional Order Integral-Tilt Derivative Controller for Frequency Regulation of Interconnected Diverse Renewable Energy Resources," *IEEE Access*, vol. 10, pp. 43514–43527, 2022, doi: 10.1109/ACCESS.2022.3167811.

[50] M. G. M. Abdolrasol, S. M. S. Hussain, T. S. Ustun, M. R. Sarker, M. A. Hannan, R. Mohamed, J. A. Ali, S. Mekhilef, and A. Milad, "Artificial Neural Networks Based Optimization Techniques: A Review," *Electronics*, vol. 10, 2021, doi: 10.3390/electronics10212689.

[51] Y.-J. Liu, W. Zhao, L. Liu, D. Li, S. Tong, and C. L. P. Chen, "Adaptive Neural Network Control for a Class of Nonlinear Systems With Function Constraints on States," *IEEE Transactions on Neural Networks and Learning Systems*, vol. 34, no. 6, pp. 2732–2741, 2023, doi: 10.1109/TNNLS.2021.3107600.

[52] E. Viera-Martin *et al*., "Artificial neural networks: a practical review of applications involving fractional calculus," *European Physical Journal Special Topics*, vol. 231, pp. 2059–2095, 2022, doi: 10.1140/epjs/s11734-022-00455-3.

[53] T. K. Gupta and K. Raza, "Optimizing Deep Feedforward Neural Network Architecture: A Tabu Search Based Approach," *Neural Processing Letters*, vol. 51, pp. 2855–2870, 2020, doi: 10.1007/s11063-020-10234-7.

[54] N. B. Shaik, S. R. Pedapati, S. A. A. Taqvi, A. R. Othman, and F. A. A. Dzubir, "A Feed-Forward Back Propagation Neural Network Approach to Predict the Life Condition of Crude Oil Pipeline," *Processes*, vol. 8, 2020, doi: 10.3390/pr8060661.

[55] M. M. Hammad, "Deep Learning Activation Functions: Fixed-Shape, Parametric, Adaptive, Stochastic, Miscellaneous, Non-Standard, Ensemble," *arXiv preprint*, 2024, doi: 10.48550/arXiv.2407.11090.

[56] S. Y. Heng, W. M. Ridwan, P. Kumar, et al., "Artificial neural network model with different backpropagation algorithms and meteorological data for solar radiation prediction," *Scientific Reports*, vol. 12, 2022, doi: 10.1038/s41598-022-13532-3.

[57] M. Dampfhoffer, T. Mesquida, A. Valentian, and L. Anghel, "Backpropagation-Based Learning Techniques for Deep Spiking Neural Networks: A Survey," *IEEE Transactions on Neural Networks and Learning Systems*, vol. 35, no. 9, pp. 11906–11921, 2024, doi: 10.1109/TNNLS.2023.3263008.

[58] T. Li, G. Kou, and Y. Peng, "Improving malicious URLs detection via feature engineering: Linear and nonlinear space transformation methods," *Information Systems*, vol. 91, 2020, doi: 10.1016/j.is.2020.101494.

[59] L. Li and M. Thornton, *Digital System Verification: A Combined Formal Methods and Simulation Framework*, Springer Nature, 2022, doi: 10.1007/978-3-031-79815-3.

[60] J. N. Chukwunweike *et al*., "Integrating deep learning, MATLAB, and advanced CAD for predictive root cause analysis in PLC systems: A multi-tool approach to enhancing industrial automation and reliability," *World Journal of Advance Research and Review*, vol. 23, no. 2, pp. 1778–1790, 2024, doi: 10.30574/wjarr.2024.23.2.2631.

[61] N. F. Ibrahim, M. M. Mahmoud, H. Alnami, D. E. M. Wapet, S. A. Ardjoun, M. I. Mosaad, A. M. Hassan, and H. Abdelfattah, "A new adaptive MPPT technique using an improved INC algorithm supported by fuzzy self-tuning controller for a grid-linked photovoltaic system," *PLoS One*, vol. 18, no. 11, p. e0293613, 2023, doi: 10.1371/journal.pone.0293613.

[62] W. Hanini and M. Ayadi, "PSpice and Simulink co-simulation for diode and AC-DC converter using SLPS interface software," *2017 18th International Conference on Sciences and Techniques of Automatic Control and Computer Engineering (STA)*, pp. 408-413, 2017, doi: 10.1109/STA.2017.8314910.

[63] Y. Wang, Y. Zhang, H. Yang, and J. Rodriguez, "Variable-vector-based model predictive control with reduced current harmonic and controllable switching frequency for PMSM drives," *IEEE Transactions on Power Electronics*, vol. 39, no. 12, pp. 16429–16441, 2024, doi: 10.1109/TPEL.2024.3441726.

[64] Y. Gao, S. Wang, T. Dragicevic, P. Wheeler, and P. Zanchetta, "Artificial intelligence techniques for enhancing the performance of con-

trollers in power converter-based systems—An overview," *IEEE Open Journal of Industry Applications*, vol. 4, pp. 366–375, 2023, doi: 10.1109/OJIA.2023.3338534.

[65] D. Chen, Z. Fang, and S. Li, "A novel BSO algorithm for three-layer neural network optimization applied to UAV edge control," *Neural Processing Letters*, vol. 55, pp. 6733–6752, 2023, doi: 10.1007/s11063-023-11157-9.

[66] L. S. Pusztaházi, G. Eigner, and O. Csiszár, "Parametric activation functions for neural networks: A tutorial survey," *IEEE Access*, vol. 12, pp. 168626–168644, 2024, doi: 10.1109/ACCESS.2024.3474574.

[67] B. Stojanović, S. Gajević, N. Kostić, S. Miladinović, and A. Vencl, "Optimization of parameters that affect wear of A356/Al_2O_3 nanocomposites using RSM, ANN, GA and PSO methods," *Industrial Lubrication and Tribology*, vol. 74, no. 3, pp. 350–359, 2022, doi: 10.1108/ILT-07-2021-0262.

[68] A. A. Asiri, A. Shaf, T. Ali, M. Aamir, M. Irfan, and S. Alqahtani, "Enhancing brain tumor diagnosis: an optimized CNN hyperparameter model for improved accuracy and reliability," *PeerJ Computer Science*, vol. 10, 2024, doi: 10.7717/peerj-cs.1878.